

A broadband X-ray imaging spectroscopy in the 2030s: the FORCE mission

Koji Mori^a, Takeshi G. Tsuru^b, Kazuhiro Nakazawa^c, Yoshihiro Ueda^d, Shin Watanabe^e, Takaaki Tanaka^f, Manabu Ishida^e, Hironori Matsumoto^g, Hisamitsu Awaki^h, Hiroshi Murakamiⁱ, Masayoshi Nobukawa^j, Ayaki Takeda^a, Yasushi Fukazawa^k, Hiroshi Tsunemi^g, Tadayuki Takahashi^l, Ann Hornschemeier^m, Takashi Okajima^m, William W. Zhang^m, Brian J. Williams^m, Tonia Venters^m, Kristin Madsen^{m,n}, Mihoko Yukita^{m,o}, Hiroki Akamatsu^p, Aya Bamba^q, Teruaki Enoto^r, Yutaka Fujita^s, Akihiro Furuzawa^t, Kouichi Hagino^u, Kosei Ishimura^v, Masayuki Itoh^w, Tetsu Kitayama^x, Shogo Kobayashi^y, Takayoshi Kohmura^z, Aya Kubota^{aa}, Misaki Mizumoto^d, Tsunefumi Mizuno^k, Hiroshi Nakajima^u, Kumiko K. Nobukawa^{ab}, Hirofumi Noda^g, Hirokazu Odaka^q, Naomi Ota^{ac}, Toshiki Sato^{ad}, Megumi Shidatsu^h, Hiromasa Suzuki^f, Hiromitsu Takahashi^k, Atsushi Tanimoto^{af}, Yukikatsu Terada^{ae}, Yuichi Terashima^h, Hiroyuki Uchida^b, Yasunobu Uchiyama^{ad}, Hiroya Yamaguchi^e, and Yoichi Yatsu^{ag}

^aDepartment of Applied Physics and Electronic Engineering, University of Miyazaki, Miyazaki 889-2192, Japan

^bDepartment of Physics, Kyoto University, Kyoto 606-8502, Japan

^cDepartment of Physics, University of Tokyo, Tokyo 113-0033, Japan

^dDepartment of Astronomy, Kyoto University, Kyoto 606-8502, Japan

^eInstitute of Space and Astronautical Science (ISAS), Japan Aerospace Exploration Agency (JAXA), Kanagawa 252-5210, Japan

^fDepartment of Physics, Konan University, Hyogo 658-8501, Japan

^gDepartment of Earth and Space Science, Osaka University, Osaka 560-0043, Japan

^hDepartment of Physics, Ehime University, Ehime 790-8577, Japan

ⁱDepartment of Information Science, Faculty of Liberal Arts, Tohoku Gakuin University, Miyagi 981-3193, Japan

^jDepartment of Teacher Training and School Education, Nara University of Education, Nara 630-8528, Japan

^kDepartment of Physical Science, Hiroshima University, Hiroshima 739-8526, Japan

^lKavli Institute for the Physics and Mathematics of the Universe (WPI), The University of Tokyo, Chiba, 277-8583, Japan

^mNASA's Goddard Space Flight Center, Greenbelt, MD 20771, USA

ⁿCRESST, Department of Physics, and Center for Space Science and Technology, UMBC, Baltimore, MD 21250, USA

^oThe Johns Hopkins University, Homewood Campus, Baltimore, MD 21218, USA

^pSRON Netherlands Institute for Space Research, 3584 CA Utrecht, The Netherlands

^qDepartment of Physics, The University of Tokyo, Tokyo, 113-0033, Japan

^rExtreme natural phenomena RIKEN Hakubi Research Team, Cluster for Pioneering Research, RIKEN, Saitama 351-0198, Japan

^sDepartment of Physics, Tokyo Metropolitan University, Tokyo 192-0397, Japan

^tFujita Health University, Aichi 470-1192, Japan

^uCollege of Science and Engineering, Kanto Gakuin University, Kanagawa 236-8501, Japan

^vFaculty of Science and Engineering, Waseda University, Tokyo 169-8555, Japan

^wDepartment of Human Environmental Science, Kobe University, Hyogo 657-8501, Japan

^xDepartment of Physics, Toho University, Chiba 274-8510, Japan

^yDepartment of Physics, Tokyo University of Science, Tokyo 162-8601, Japan

^zDepartment of Physics, Tokyo University of Science, Chiba 278-8510, Japan

^{aa}Department of Electronic Information Systems, Shibaura Institute of Technology, Saitama 337-8570, Japan

^{ab}Department of Science, Kindai University, Osaka 577-8502, Japan

^{ac}Department of Physics, Nara Women's University, Nara 630-8506, Japan

^{ad}Department of Physics, Rikkyo University, Tokyo 171-8501, Japan

^{ae}Graduate School of Science and Engineering, Saitama University, Saitama, 338-8570, Japan

^{af}Graduate School of Science and Engineering, Kagoshima University, Kagoshima, 890-8580, Japan

^{ag}Department of Physics, Tokyo Institute of Technology, Tokyo 152-8551, Japan

ABSTRACT

In this multi-messenger astronomy era, all the observational probes are improving their sensitivities and overall performance. The Focusing on Relativistic universe and Cosmic Evolution (FORCE) mission, the product of a JAXA/NASA collaboration, will reach a 10 times higher sensitivity in the hard X-ray band ($E > 10$ keV) in comparison with any previous hard X-ray missions, and provide simultaneous soft X-ray coverage. FORCE aims to be launched in the early 2030s, providing a perfect hard X-ray complement to the ESA flagship mission Athena. FORCE will be the most powerful X-ray probe for discovering obscured/hidden black holes and studying high energy particle acceleration in our Universe and will address how relativistic processes in the universe are realized and how these affect cosmic evolution. FORCE, which will operate over 1–79 keV, is equipped with two identical pairs of supermirrors and wideband X-ray imagers. The mirror and imager are connected by a high mechanical stiffness extensible optical bench with alignment monitor systems with a focal length of 12 m. A light-weight silicon mirror with multi-layer coating realizes a high angular resolution of $< 15''$ in half-power diameter in the broad bandpass. The imager is a hybrid of a brand-new SOI-CMOS silicon-pixel detector and a CdTe detector responsible for the softer and harder energy bands, respectively. FORCE will play an essential role in the multi-messenger astronomy in the 2030s with its broadband X-ray sensitivity.

Keywords: FORCE, broadband X-ray imaging spectroscopy, black hole, particle acceleration, supernova explosion, silicon mirror, SOI-CMOS, CdTe

1. INTRODUCTION

What is the ultimate goal of astrophysics? The simplest answer is to understand how the Universe works — how it started, how it has evolved into the present shape, how it will ultimately be. We seek to learn what physical laws govern both the Universe and its contents. These are big topics, requiring that we observe all aspects of the Universe by all the methods we have available. The concept of our proposing mission is to focus on the high energy processes that govern much of the structure formation and evolution of the Universe by means of highly sensitive wideband X-ray observations.

High energy phenomena are ubiquitously seen at all levels of the hierarchical structure of the Universe, from the largest gravitationally bound structures, galaxy clusters, down to the scale of individual stars, in stellar explosions and in the remnants of those explosions, including black holes. These high energy phenomena play crucial roles in the structure formation and evolution of the Universe as we can trace particle acceleration

Further author information: (Send correspondence to K.M.)

K.M.: E-mail: mori@astro.miyazaki-u.ac.jp, Telephone: 81 985 58 7371

that affects how large structures form and the supermassive black holes that are apparently coevolving with galaxies over cosmic time.

These phenomena provide us with rich information concerning physical processes working in the most extreme conditions, bringing dramatic deviations from equilibrium states of the Universe. By understanding such extreme conditions, we also verify the underlying physical conditions. Highly sensitive wideband X-ray observations have a great advantage to study these high energy phenomena providing sensitivity to both thermal emission from plasmas with temperatures of a few million Kelvin (such as may be present in accretion disks around black holes) as well as non-thermal emission (created by particle acceleration). There is a particular opportunity at energies above 10 keV, where only very limited exploration has occurred to date: highly-sensitive observations at these energies have the potential to unveil the hidden Universe underneath thick, dense surrounding materials and/or in the presence of overwhelming thermal emission that confuses observations at energies below 10 keV.

The Focusing on Relativistic universe and Cosmic Evolution (FORCE) mission^{1,2} is the product of a JAXA/NASA collaboration and aims to be launched in the early 2030s. FORCE will reach a 10 times higher sensitivity in the hard X-ray band ($E > 10$ keV) in comparison with any previous hard X-ray missions and provide simultaneous soft X-ray coverage. The science goal of the FORCE mission is to understand how relativistic processes in the universe are realized and how these affect cosmic evolution. In this paper, we describe FORCE’s scientific objectives, current design overview, and roles in multi-messenger astronomy era.

2. SCIENTIFIC OBJECTIVES

We summarize the scientific goal into three scientific objectives as follows:

1. How black holes grow and how they affect galaxy evolution,
2. How non-thermal energy is generated and how much non- thermal energy is contained in the universe, and
3. How stars evolve and explode.

In this section, the three scientific objectives are reviewed.

2.1 How black holes grow and how they affect galaxy evolution

2.1.1 Supermassive Black Hole: Co-evolution with their host galaxies

Nearly all galaxies in the universe contain supermassive black holes (SMBHs) in their centers, whose masses range from $\sim 10^5$ to $10^{10} M_{\odot}$. Moreover, a tight correlation between the masses of the central SMBHs and the masses of galactic stellar bulges has been reported.³ These facts indicate that the formation process of SMBHs and that of galaxies are strongly coupled to each other, despite the large difference in their physical sizes (>8 orders of magnitude). Thus, it is one of the most fundamental questions in modern astronomy how these SMBHs in galactic centers formed and “co-evolved” with their host galaxies over the history of the Universe.

A key population for understanding the origin of the coevolution of galaxies and SMBHs is the most heavily obscured Active Galactic Nuclei (AGNs), whose line-of-sight hydrogen column density, N_{H} , is larger than 10^{24} , so-called Compton-thick AGNs (CTAGNs). According to the current best understanding, major mergers of galaxies trigger violent star formation and intense mass accretion onto SMBHs deeply “buried” by surrounding gas and dust. This means that a key aspect of growth of SMBHs, the merging process, is largely hidden at most electromagnetic wavelengths. Luckily, it is visible at energies above 10 keV. In fact, NuSTAR has shown $>50\%$ of late-stage AGN mergers in the local Universe are Compton-thick,⁴ indicating that CTAGNs may be a distinct population from normal AGNs, harboring much missing information about merger growth. Thus, these CTAGNs (or buried AGNs) are unique tracers of the key processes for understanding the coevolution, i.e., merger and subsequent rapid growth of SMBHs. However, the basic questions on CTAGNs remain open: (1) how many CTAGNs, largely missing from the current census, are present in the Universe and (2) what is the contribution of CTAGNs to the total growth of SMBHs (merger, accretion, or both?).

Hard X-ray surveys at energies above 10 keV provide the least biased AGN sample as they have the strong penetrating power to overcome obscuration. However, due to technical challenges, most of the previous X-ray surveys with good image quality were performed in energy bands below 10 keV, which were insufficient to catch the primary emission component from CTAGNs. There have been all-sky hard X-ray surveys above ~ 10 keV with non-focusing optics with Swift/BAT and INTEGRAL. These surveys have found a part of the CTAGN population in the local universe. However, their cosmological evolution requires a census to fainter populations with a true focused imaging hard X-ray survey.

The first such imaging survey was conducted by the NuSTAR mission beginning in 2012. NuSTAR has arcminute angular resolution and has been an excellent pathfinder for the FORCE mission, having resolved $\sim 35\%$ of the cosmic X-ray background (CXB) in the 8–24 keV band.⁵ This CXB, X-ray emission that is pervasive over the entire sky, represents the integrated emission from accreting SMBHs over cosmic time. Buried within this signal, we expect to find a population of CTAGNs. NuSTAR has provided us with new insights on CTAGN populations, implying that there may be far more CTAGNs than those assumed in canonical AGN population synthesis models.^{6,7} However, much deeper hard X-ray surveys, with >10 times better sensitivities than NuSTAR ($\sim 3 \times 10^{-15}$ erg cm⁻² s⁻¹ in the 10–40 keV band), must be conducted to determine the evolution of CTAGNs over cosmic time and thus finally provide a complete picture of how SMBH growth occurs over the history of the Universe.

2.1.2 Intermediate-mass Black Hole: Nature of ultraluminous X-ray sources

Central SMBHs in galaxies must have grown, via mergers and/or accretion, from lighter “seed” black holes. Thus, another key population for understanding formation mechanisms of SMBHs is that of intermediate-mass black holes (IMBHs), those with masses of $\sim 10^{2-4} M_{\odot}$. The origin of IMBHs is fundamentally important, connecting SMBHs to lower mass black holes: IMBHs may be remnants of population III stars or even primordial black holes that formed just after the Big Bang. We expect that some fraction of this IMBH population to remain inside galaxies in the relatively local Universe today (e.g., those which did not undergo growth via either merger or accretion to become SMBH). The gravitational wave interferometers LIGO and VIRGO revealed the presence of black holes with masses (up to $80 M_{\odot}$) considerably larger than ordinary stellar-mass ($\sim 5\text{--}15 M_{\odot}$) black holes. However, to date, there is no truly convincing example of IMBHs in the $10^{2-4} M_{\odot}$ range. Identifying more IMBHs over a wide mass range will provide strong constraints on theories of black hole evolution in the Universe.

When BHs accrete matter from their surroundings, they can be observed as luminous X-ray emitters because the Eddington limit (the luminosity where the gravitational force is balanced by radiation pressure) is nominally proportional to the black hole mass. Ultra-Luminous X-ray sources (ULXs), off-nucleus compact X-ray sources found in other galaxies with typical luminosities of 10^{39-40} erg s⁻¹ provide a useful population for studying possible IMBHs (e.g., Ref.8). Although some ULXs have turned out to harbor neutron stars^{9,10} and many likely host Stellar-mass Black Holes (StMBHs), the nature of the majority (> 400 sources including candidates; Ref.11) is yet to be investigated with sufficiently sensitive hard ($E > 10$ keV) X-ray observations because those are still too dim for instruments currently available above 10 keV. While most ULXs may be stellar-mass objects accreting at extreme rates which are also worth studying in terms of accretion growth of black holes, it is possible that a handful of them are IMBHs hidden within the ULX population. Of particular importance is to look for the hard X-ray emission above 10 keV, as the peak hard X-ray luminosity has long been proposed to be a BH-neutron star discriminator.¹² We will specifically search for hard X-ray emission from ULX sources in globular clusters and satellite galaxies around giant elliptical galaxies as well as in dwarf elliptical galaxies where the central black holes are likely to be of intermediate mass.

2.1.3 Stellar-mass Black Hole: Missing population in our Galaxy

To reveal the connection between the IMBHs and “ordinary” StMBHs produced by core collapses of massive stars, we need to first establish statistical properties of StMBHs, which are much less luminous than ULXs. The Milky Way galaxy is an excellent target for these studies. It has been posited that 100 million StMBHs may have formed within the Milky Way over its 10-billion-year lifetime.¹³ Among them, only a few tens of bright ($L_X > 10^{36}$ erg s⁻¹) X-ray binary systems that contain black holes are currently known, most of which

are transients.¹⁴ Thus, most of StMBHs in the Milky Way galaxy are missing. The present sample is too small to constrain the true underlying mass function and spatial distribution.

It is expected that StMBHs (either isolated or in binary systems) with low mass-accretion rates are observed as much less luminous X-ray sources than the X-ray transients. For example, the estimated X-ray emission from a single (non-binary) black hole present within the interstellar medium is very small ($< 10^{34}$ erg s⁻¹; e.g., Ref.15). It is possible some of the extremely faint isolated stellar mass black holes have already been found, but without hard band ($E > 10$ keV) coverage, it is impossible to distinguish from other sources. Chandra performed a deep survey in the Galactic Center region and detected 9,000 sources with $L_X > 10^{31}$ erg s⁻¹.¹⁶ Although the majority of these sources are thought to be white dwarf binaries,¹⁷ some should be StMBHs whose identifications are currently impossible. White dwarf binaries have optically thin thermal emission with 100 million K, whereas low luminosity StMBHs must show power law spectra with a typical photon index of ~ 1.5 from the advection dominated accretion flows. To differentiate between them, measuring broadband X-ray spectra that cover energies above 10 keV is critical. The sensitivity of current instruments is limited to those with $L_X > 10^{33}$ erg s⁻¹, missing the bulk of the population and making statistical studies impossible.

2.2 How non-thermal energy is generated and how much non- thermal energy is contained in the universe

According to the current particle acceleration paradigm, thermal particles with a Maxwell-Boltzmann distribution attain high energies through diffusive shock acceleration (or DSA, also known as first-order Fermi acceleration; see e.g., Ref.18) which may occur at supernova shocks. This paradigm has been successful in producing nonthermal, power-law energy spectra for the distribution of accelerated particles, consistent with high-energy spectral measurements in a variety of astrophysical systems, including SNRs. However, key details about the DSA process have remained elusive for decades, particularly whether and to what extent thermal particles are accelerated to nonthermal energies, and how efficient the process is.

In this regard, it is quite important to measure the total amount and the spectra of sub-relativistic particles. Nonthermal bremsstrahlung in the hard X-ray energy range is a promising emission channel to probe such particles. Recently, a NuSTAR observation revealed hard X-ray emission in the SNR W49B, which was attributed to nonthermal bremsstrahlung from electrons.¹⁹ Such observations are already challenging for the DSA process, as they pointed to either the presence of a population of sub-relativistic particles or much more efficient particle acceleration than predicted in the DSA paradigm. However, with its backgrounds and angular resolution, NuSTAR was unable to provide precise measurements of the amount of accelerated particles emitting in this band or their spectrum. Both lower detector backgrounds and more efficient exclusion of cosmic X-ray background are necessary to more precisely measure the spectrum of the particles emitting in the hard X-ray band, particularly at the transition from the thermal part of the spectrum to the nonthermal part that is inaccessible to instruments less sensitive in the hard X-ray band. Detailed spatial information for the hard X-ray emission is also important for comparison with maps of the ambient gas. This will prove essential for translating the luminosity of the nonthermal bremsstrahlung to the total amount of particles radiating in that band.

In clusters of galaxies, particle acceleration may be studied in a manner similar to the methods outlined for SNRs. From radio observations of synchrotron emission, we know that relativistic particles with energies about 10^9 eV have to be accelerated even in outer regions of clusters because their life is on the order of 10^9 yr. In order to separately constrain the magnetic fields and the energy density of particles in intracluster environments, measurements of the energy spectrum and image of inverse Compton emission from clusters of galaxies are essential. Inverse Compton emission arises when relativistic electrons (with energies of 10^9 eV) scatter 2.7 K microwave background photons and raise the photon energy to X-ray energies. The measurement needs to be done above ~ 10 keV, where the inverse Compton component is stronger than the thermal emission of the intracluster gas. These data will tell us the energy density and spectrum of electrons. The combination of the hard X-ray and radio data will solve the degeneracy between magnetic field and electrons, giving us the magnetic field strength without further assumption.

There are a few clusters of galaxies with exceptionally high temperature of about 25 keV detected with Chandra and Suyaev-Zel'dovich measurements: RX J1347.5-1145²⁰ ($z=0.451$) and 1E0657-56²¹ ($z=0.296$).

Existence of very hot clusters at a fairly distant Universe can be a challenge to the cold dark matter scenario of structure formation (e.g., Ref.22), since the bottom-up process can build up the mass to a certain limit within the cosmological time scale. The high sensitivity observations in the high energy X-ray band will enable us to determine ICM temperatures precisely for a wide range of clusters, and the current scenario of the structure formation will be critically examined based on a sample of the hottest clusters.

2.3 How stars evolve and explode

Type Ia supernova explosions are caused either by mass accretion of a white dwarf from a stellar companion or merger of two white dwarfs forming a binary system. In both scenarios, one of the important questions is whether supernovae occur with the exploding white dwarf mass close to the Chandrasekhar limit ($\sim 1.4 M_{\odot}$) or well below the limit. One of the most powerful diagnostic tools for disentangling the two cases is nickel-to-iron (Ni/Fe) mass ratio^{23,24}. In the case of the Chandrasekhar limit case, the core of the white dwarf can be dense enough for the electron capture process to efficiently take place, resulting in more abundant neutron-rich species including Ni. The Ni/Fe mass ratio can be measured using K-shell transition lines of the elements, which appear at $\sim 6-8$ keV.

Recent theoretical studies suggest that asymmetry is a key ingredient to make core-collapse supernovae explode.²⁵⁻²⁸ Therefore, measurements of the asymmetry can strongly constrain the models for core-collapse supernova explosions. We aim to do so based on observations of line emissions from radioactive decay of ^{44}Ti at 68 keV and 78 keV. Synthesized in the innermost part of supernova ejecta, both the total amount synthesized and distribution of ^{44}Ti serves as one of the most powerful probes of asymmetry of core-collapse supernovae.

3. MISSION DESIGN OVERVIEW

3.1 Mission requirement on angular resolution

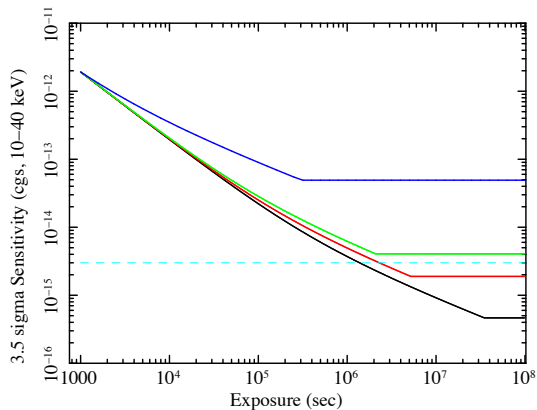


Figure 1. Point source sensitivity as a function of exposure time in deep surveys for CTAGNs. Black, red, green colors indicate those for $10''$, $15''$, and $20''$ HPD cases, respectively, while blue color shows the Hitomi case. A cyan dashed line indicates the scientific requirement described in Sec. 2.1.1.

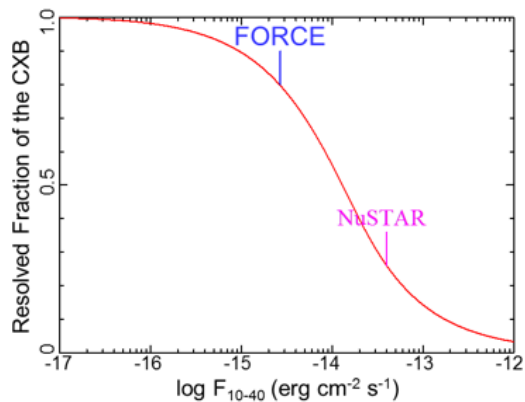


Figure 2. Resolved fraction of the CXB in the 10–40 keV band as a function of flux limit predicted by a standard population synthesis model.²⁹

The scientific objectives described in the previous section require unprecedented high sensitivity in the hard X-ray band above 10 keV for both point and diffuse sources. The most stringent requirement on sensitivity comes from the deep surveys for CTAGNs. The deep surveys need highest sensitivity for the faintest point sources, obscured and distant AGNs. As a bi-product, detection/exclusion of such sources effectively reduces systematic uncertainty in the background estimation for diffuse sources due to CXB fluctuation, resulting in

higher sensitivity for diffuse sources. Therefore, roughly speaking, all other science requirements on sensitivity are met by the requirement from the deep surveys for CTAGNs.

As described in Sec. 2.1.1, a sensitivity limit of 3×10^{-15} erg cm⁻² s⁻¹ in the 10–40 keV band is the threshold defined by the deep surveys for CTAGNs. In order to reach this limit, the most important design parameter is angular resolution. Fig. 1 shows sensitivity curves (sensitivity reached at a given exposure time) with several angular resolution cases. Here, the half power diameter (HPD) of the point spread function (PSF) is used as a measure of angular resolution. In any cases, in the short exposure regime less than 100 ks, the sensitivity increases as the exposure time increases. However, at some point, the sensitivity never gets better due to confusion of faint sources no matter how much exposure time is invested. The sensitivity limit of 3×10^{-15} erg cm⁻² s⁻¹ requires that the angular resolution must be better than 15". Fig. 2 shows the resolved fraction of the CXB in the 10–40 keV band as a function of flux limit predicted by a standard population synthesis model.²⁹ The FORCE's sensitivity limit makes it possible to resolve $\sim 80\%$ of the hard CXB into discrete sources, meaning that we will be able to finally perform a thorough census of all the accreting SMBHs in the universe. At the same time, we will be able to understand the role of major mergers for SMBH growth, and hence the origin of the coevolution.

3.2 Mission and instrument design



Figure 3. Schematic view of the FORCE satellite.

Table 1. Instrument parameters

Angular resolution (HPD)	<15"
Multi-layer Coating	Pt/C
Field of view (50% response) at 30 keV	>7' × 7'
Effective Area at 30 keV	230 cm ²
Energy range	1–79 keV
Energy resolution (FWHM) at 6 keV	<300 eV
Instrument background	comparable to those of Hitomi HXI ³⁰
Timing resolution (absolute)	several × 10 μs

Fig. 3 shows a schematic view of the FORCE satellite, and Table 1 summarizes key instrument parameters. The overall mission design is determined by scientific requirements, technical heritage of our previous mission, *Hitomi*, and restrictions from the launch vehicle. The weight of the FORCE satellite is about 1 metric ton, and is planned to be launched into a circular orbit with altitude of 500–600 km and inclination angle of 31 degrees

or less by an ISAS/JAXA solid-propellant Epsilon-S rocket. FORCE carries co-aligned, two identical pairs of a supermirror with high angular resolution and a focal-plane detector with broadband X-ray response. The supermirror and detector are separated by a focal length of 12 m. The long focal length is essential to keep sufficient effective area for hard X-ray, requiring an extendable optical bench (EOB) that can be stowed to fit in the launch fairing and deployed on-orbit. Lateral displacements of the detector in the alignment plane due to the thermal distortion of the EOB are monitored by a laser metrology system³¹ in instantaneous fashion, and the position reconstruction of detected X-rays are performed on ground on a photon-by-photon basis. The precision of this system affects the net angular resolution we finally obtain. In the case of *Hitomi*, the movement in the alignment plane was less than 400 μm with a focal length of 12 m.³² We fully utilize the *Hitomi* heritages in our system.

3.2.1 X-ray supermirror based on light-weight, high-resolution silicon mirror

The mirror substrates of our X-ray supermirrors are made based on the single-crystal silicon mirror technology, which has been in development at NASA’s Goddard Space Flight Center.³³ X-ray mirror technologies are generally evaluated from three aspects: angular resolution, mass per unit effective area, and cost per unit effective area. Especially, budgetary-limited small missions need to find the best compromise among these aspects, or rather focus on the latter two. The single-crystal silicon mirror technology simultaneously meets the three-fold requirement. Maturing processes toward a flight-ready X-ray mirror assembly are extensively tested.

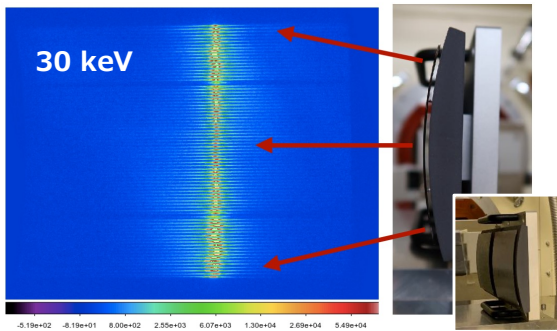


Figure 4. Reflected X-ray images obtained in a raster scan measurement with 30 keV X-ray beam. A silicon mirror module of a pair of the primary and secondary segments was tested, whose picture is shown in the inset.

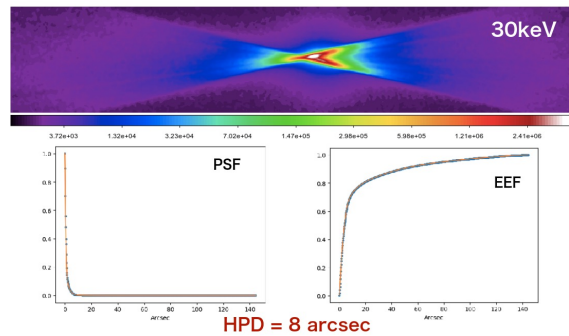


Figure 5. Summed image obtained from the raster scan measurement shown in Fig. 4 (top). The PSF (bottom left) and EEF (bottom right) are derived from the summed image.

We have been measuring X-ray performances of a multi-layer coated single-crystal silicon mirror. FORCE will use the Wolter-I optical prescription, in which the primary mirror is parabolic and the secondary mirror is hyperbolic in shape. A silicon mirror module of a pair of the primary and secondary segments was made for test purpose as shown in Fig. 4 inset. The mirrors were coated with Pt/C depth-graded multi-layers following a method used for the *Hitomi* hard X-ray mirror.³⁴ We carried out the characterization of the module at the synchrotron facility SPring-8 BL20B2, where we can illuminate the module with a monochromatic, hard X-ray parallel beam. Fig. 4 shows the result of a raster scan measurement with the 30 keV X-ray beam. The reflected X-ray images slightly differ according to position, but are well sorted. Fig. 5 shows a summed image, and the PSF and encircled energy function (EEF) derived from the summed image. The HPD of $\sim 8''$ was obtained in this measurement. Although this result is from a single pair of the primary and secondary segments, this value is well below the mission requirement.

3.2.2 Wideband hybrid X-ray imager

Fig. 6 shows a schematic drawing of the FORCE’s focal plane detector, Wideband Hybrid X-ray Imager (WHXI). The WHXI is a descendant of the Hard X-ray Imager (HXI) onboard *Hitomi*,³⁵ sharing a concept that Si and CdTe hybrid detector surrounded by BGO active shield. The upper Si sensor is responsible for incoming soft X-ray detection whereas the lower CdTe sensor receives hard X-rays passing through the Si

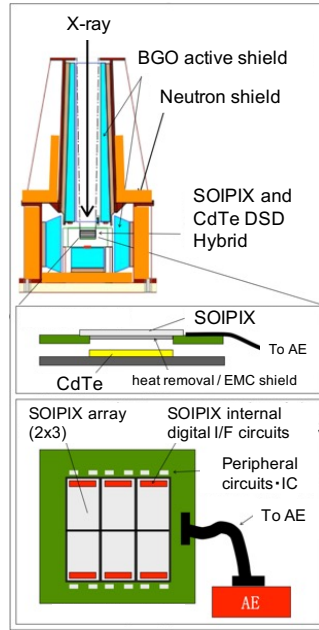


Figure 6. Schematic drawing of WHXI

sensor, realizing broadband X-ray response. What is new in the WHXI is to use a single layer of the SOI-CMOS pixel detector (SOIPIX)³⁶ for the Si sensor in place of four layers of the double-sided Si strip detector (DSSD) used in the HXI. Lower readout noise and better energy resolution of SOIPIX in comparison with the DSSD can lower the energy threshold down to 1 keV and allow us to perform X-ray line diagnostics in the Fe band around 6 keV. SOIPIX is also equipped with a self-trigger function and fast response of $< 10 \mu\text{s}$ so that the anti-coincidence technique can be applied as in the case of the DSSD in the HXI. A single SOIPIX chip has a dimension of $22 \text{ mm} \times 14 \text{ mm}$. In the WHXI, six SOIPIX chips are arranged in a 2×3 grid, resulting in an imaging area size of $44 \text{ mm} \times 44 \text{ mm}$ with gaps between chips as shown in Fig. 6. With a focal length of 12 m, this number corresponds to a 12.5×12.5 field of view. The CdTe DSD has a dimension of $30 \text{ mm} \times 30 \text{ mm}$, covering a 8.5×8.5 field of view. Since the supermirror has an energy-dependent vignetting function and provides a larger field of view in lower energy band, soft X-ray responsible SOIPIX has a larger spatial coverage. We plan to operate the WHXI with a working temperature of $-25 \pm 1 \text{ }^\circ\text{C}$.

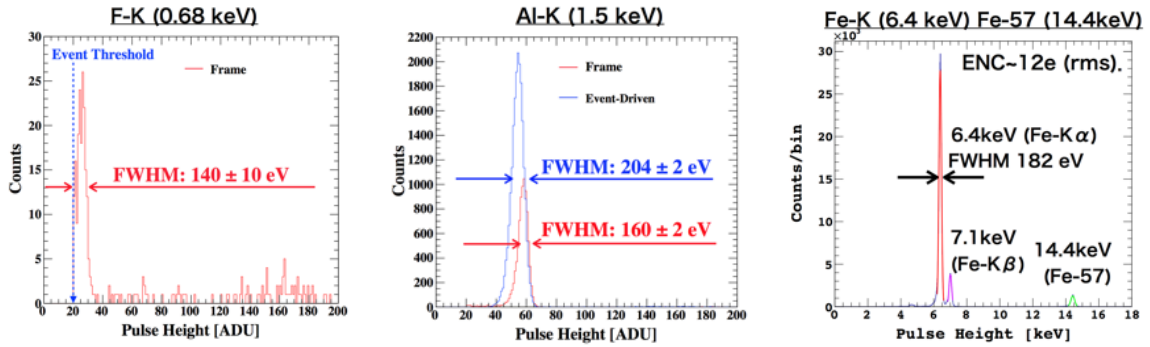


Figure 7. X-ray spectra taken with SOIPIX at 0.68 keV (left), 1.5 keV (middle), and 6.4 keV (right). Note that the spectrum at 0.68 keV is taken with the frame mode, not with the event-driven mode.³⁷

Fig. 7 shows the current X-ray spectroscopic performance of SOIPIX. Please note that these spectra were taken with a small size chip. Nonetheless, the energy resolution at 6.4 keV is close to that of X-ray CCD. Al-K X-rays at 1.5 keV were successfully detected with the event-driven readout, but F-K X-rays at 0.68 keV

were not.³⁷ Further studies in the reduction of readout noise are ongoing.

4. ROLES IN MULTI-MESSENGER ASTRONOMY ERA IN THE 2030S

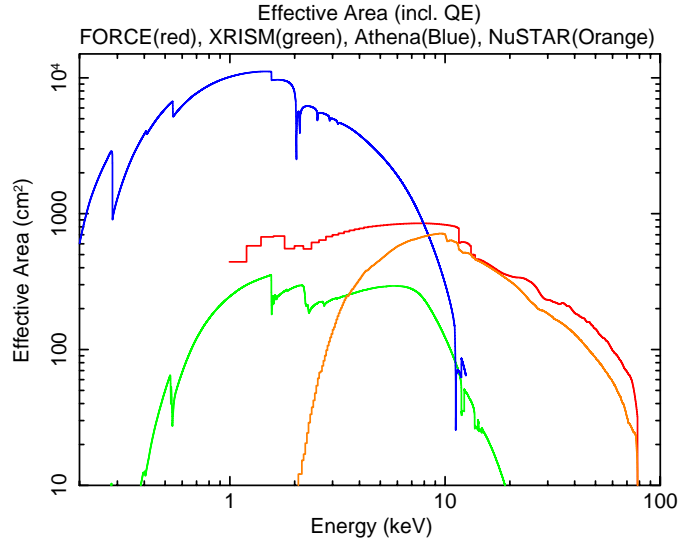


Figure 8. Comparison of effective area among FORCE (red), NuSTAR (orange), XRISM (green), and Athena (blue).

Fig. 8 shows an effective area of FORCE as well as those of NuSTAR, XRISM, and Athena. In comparison with NuSTAR, FORCE is characterized by an enhancement of the effective area in soft X-ray band below 10 keV, providing simultaneous broad band coverage without coordinated observations with other observatories. XRISM, Japan’s seventh X-ray astronomy mission to be launched in the Japanese fiscal year 2022, is expected to revolutionize our understanding of the X-ray Universe with its unprecedented energy resolution. Athena will follow and expand the high resolution spectroscopy in 2030s. The Athena design is optimized to have a large effective area in the soft X-ray band around 1 keV, which is in clear contrast with that of FORCE, and therefore FORCE and Athena are quite complementary to each other in 2030s.

Hard X-ray studies are also complementary to current and future gravitational wave studies. Gravitational waves provide a useful way to find IMBHs that grow via mergers. LIGO, Virgo, and KAGRA will detect merging objects and are sensitive to the lower end of the IMBH range (a few hundred solar masses). LISA will sample the upper range ($> 10^4 M_{\odot}$) of IMBHs. FORCE fills in this mass gap with sensitivity over the entire range and to accreting sources (growing in a different way than mergers). Accreting IMBHs, observed as ULX or HLX sources, may only be discovered in the X-ray band, where most of their emission is radiated. LISA will also observe a significant population of Milky Way compact object binaries with wide orbits that will include StMBH. However, it will be heavily biased towards mostly white dwarf systems (e.g., Ref. 38). This LISA population of wide-orbit StMBHs will complement the FORCE population of isolated/quiescent BHs in the Galactic center to complete the full picture of StMBHs.

FORCE will also be a strong complement to TeV and neutrino observatories. Observing gamma rays in TeV energies, the Cherenkov Telescope Array (CTA) can also probe ultra-relativistic particles but with neutral pion decay emission, a different radiation channel from what we aim to detect with FORCE. In addition, future neutrino detectors would be able to detect high energy neutrino emission from SNRs, which are the decay products of charged pions. Hard X-ray data, therefore, constitute an important piece in the new field of multi-messenger astronomy. Combining hard X-ray, TeV gamma-ray, and neutrino data, we can solidly constrain the maximum acceleration energy in SNRs and can give a conclusive answer to the question about the origin of Galactic cosmic rays.

5. SUMMARY

We here present the Focusing on Relativistic universe and Cosmic Evolution (FORCE) mission, the product of a JAXA/NASA collaboration. The FORCE mission will achieve 10 times higher sensitivity in the hard X-ray band in comparison to any previous hard X-ray mission. FORCE aims to be launched in the early 2030s, as a perfect hard X-ray complement to Athena. FORCE provides broadband (1–79 keV) X-ray imaging spectroscopy with high angular resolution ($< 15''$). FORCE will be the most powerful X-ray probe for discovering obscured/hidden black holes and studying high energy particle acceleration in our Universe.

ACKNOWLEDGMENTS

The measurements of the X-ray mirror for FORCE were done at SPring-8 2018B1172, 2019B1274, and 2020A1285. This work is partially supported by JSPS KAKENHI Grant Numbers JP21H01095, JP20H00157, JP22H04572, JP21H04493, JP21H05461, JP21K18151, JP20H00175, JP19K14742.

REFERENCES

- [1] Mori, K. et al., “A broadband x-ray imaging spectroscopy with high-angular resolution: the FORCE mission,” in [*Space Telescopes and Instrumentation 2016: Ultraviolet to Gamma Ray*], den Herder, J.-W. A., Takahashi, T., and Bautz, M., eds., *Society of Photo-Optical Instrumentation Engineers (SPIE) Conference Series* **9905**, 99051O (July 2016).
- [2] Nakazawa, K. et al., “The FORCE mission: science aim and instrument parameter for broadband x-ray imaging spectroscopy with good angular resolution,” in [*Space Telescopes and Instrumentation 2018: Ultraviolet to Gamma Ray*], den Herder, J.-W. A., Nikzad, S., and Nakazawa, K., eds., *Society of Photo-Optical Instrumentation Engineers (SPIE) Conference Series* **10699**, 106992D (July 2018).
- [3] Gültekin, K. et al., “The M- σ and M-L Relations in Galactic Bulges, and Determinations of Their Intrinsic Scatter,” *ApJ* **698**, 198–221 (June 2009).
- [4] Ricci, C. et al., “BAT AGN Spectroscopic Survey. V. X-Ray Properties of the Swift/BAT 70-month AGN Catalog,” *ApJS* **233**, 17 (Dec. 2017).
- [5] Harrison, F. A. et al., “The NuSTAR Extragalactic Surveys: The Number Counts of Active Galactic Nuclei and the Resolved Fraction of the Cosmic X-Ray Background,” *ApJ* **831**, 185 (Nov. 2016).
- [6] Civano, F. et al., “The Nustar Extragalactic Surveys: Overview and Catalog from the COSMOS Field,” *ApJ* **808**, 185 (Aug. 2015).
- [7] Lansbury, G. B. et al., “The NuSTAR Serendipitous Survey: Hunting for the Most Extreme Obscured AGN at >10 keV,” *ApJ* **846**, 20 (Sept. 2017).
- [8] Makishima, K. et al., “The Nature of Ultraluminous Compact X-Ray Sources in Nearby Spiral Galaxies,” *ApJ* **535**, 632–643 (June 2000).
- [9] Bachetti, M. et al., “An ultraluminous X-ray source powered by an accreting neutron star,” *Nature* **514**, 202–204 (Oct. 2014).
- [10] Fürst, F. et al., “Discovery of Coherent Pulsations from the Ultraluminous X-Ray Source NGC 7793 P13,” *ApJ* **831**, L14 (Nov. 2016).
- [11] Walton, D. J. et al., “2XMM ultraluminous X-ray source candidates in nearby galaxies,” *MNRAS* **416**, 1844–1861 (Sept. 2011).
- [12] Barret, D. et al., “Luminosity Differences between Black Holes and Neutron Stars,” *ApJ* **473**, 963 (Dec. 1996).
- [13] Samland, M., “Modeling the Evolution of Disk Galaxies. II. Yields of Massive Stars,” *ApJ* **496**, 155–171 (Mar. 1998).
- [14] Negoro, H. et al., “The MAXI/GSC Nova-Alert System and results of its first 68 months,” *PASJ* **68**, S1 (June 2016).
- [15] Barkov, M. V., Khangulyan, D. V., and Popov, S. B., “Jets and gamma-ray emission from isolated accreting black holes,” *MNRAS* **427**, 589–594 (Nov. 2012).
- [16] Munro, M. P. et al., “A Catalog of X-Ray Point Sources from Two Megaseconds of Chandra Observations of the Galactic Center,” *ApJS* **181**, 110–128 (Mar. 2009).

- [17] Revnivtsev, M. et al., “Origin of the Galactic ridge X-ray emission,” *A&A* **452**, 169–178 (June 2006).
- [18] Bell, A. R., “The acceleration of cosmic rays in shock fronts - I.,” *MNRAS* **182**, 147–156 (Jan. 1978).
- [19] Tanaka, T. et al., “NuSTAR Detection of Nonthermal Bremsstrahlung from the Supernova Remnant W49B,” *ApJ* **866**, L26 (Oct. 2018).
- [20] Ota, N. et al., “Suzaku broad-band spectroscopy of RX J1347.5-1145: constraints on the extremely hot gas and non-thermal emission,” *A&A* **491**, 363–377 (Nov. 2008).
- [21] Markevitch, M. et al., “A Textbook Example of a Bow Shock in the Merging Galaxy Cluster 1E 0657-56,” *ApJ* **567**, L27–L31 (Mar. 2002).
- [22] Tucker, W. et al., “1E 0657-56: A Contender for the Hottest Known Cluster of Galaxies,” *ApJ* **496**, L5–L8 (Mar. 1998).
- [23] Yamaguchi, H. et al., “The Origin of the Iron-rich Knot in Tycho’s Supernova Remnant,” *ApJ* **834**, 124 (Jan. 2017).
- [24] Hitomi Collaboration, “Solar abundance ratios of the iron-peak elements in the Perseus cluster,” *Nature* **551**, 478–480 (Nov. 2017).
- [25] Blondin, J. M., Mezzacappa, A., and DeMarino, C., “Stability of Standing Accretion Shocks, with an Eye toward Core-Collapse Supernovae,” *ApJ* **584**, 971–980 (Feb. 2003).
- [26] Takiwaki, T., Kotake, K., and Suwa, Y., “A Comparison of Two- and Three-dimensional Neutrino-hydrodynamics Simulations of Core-collapse Supernovae,” *ApJ* **786**, 83 (May 2014).
- [27] Melson, T., Janka, H.-T., and Marek, A., “Neutrino-driven Supernova of a Low-mass Iron-core Progenitor Boosted by Three-dimensional Turbulent Convection,” *ApJ* **801**, L24 (Mar. 2015).
- [28] Vartanyan, D. et al., “A successful 3D core-collapse supernova explosion model,” *MNRAS* **482**, 351–369 (Jan. 2019).
- [29] Ueda, Y. et al., “Toward the Standard Population Synthesis Model of the X-Ray Background: Evolution of X-Ray Luminosity and Absorption Functions of Active Galactic Nuclei Including Compton-thick Populations,” *ApJ* **786**, 104 (May 2014).
- [30] Hagino, K. et al., “In-orbit performance and calibration of the Hard X-ray Imager onboard Hitomi (ASTRO-H),” *Journal of Astronomical Telescopes, Instruments, and Systems* **4**, 021409 (Apr. 2018).
- [31] Gallo, L. et al., “The Canadian Astro-H Metrology System,” in [*Space Telescopes and Instrumentation 2014: Ultraviolet to Gamma Ray*], **9144**, 914456 (2014).
- [32] Takahashi, T. et al., “The ASTRO-H x-ray astronomy satellite,” in [*Astronomical Telescopes and Instruments 2016 Proceeding*], *Proc. SPIE* (2016).
- [33] Zhang, W. W. et al., “Single Crystal Silicon X-ray Optics for Astronomy: high resolution, light weight, and low cost,” *Proc. SPIE*, in press (2022).
- [34] Tamura, K. et al., “Supermirror design for Hard X-Ray Telescopes on-board Hitomi (ASTRO-H),” *Journal of Astronomical Telescopes, Instruments, and Systems* **4**, 011209 (Jan. 2018).
- [35] Nakazawa, K. et al., “Hard x-ray imager onboard Hitomi (ASTRO-H),” *Journal of Astronomical Telescopes, Instruments, and Systems* **4**, 021410 (Apr. 2018).
- [36] Tsuru, T. G. et al., “Recent Progress in Development of Trigger-Output Event-Driven X-ray astronomy SOI pixel sensors,” *Proc. SPIE*, in press (2022).
- [37] Kodama, R. et al., “Low-energy x-ray performance of soi pixel sensors for astronomy, “xrpix”,” *Nuclear Instruments and Methods in Physics Research Section A: Accelerators, Spectrometers, Detectors and Associated Equipment* **986**, 164745 (2021).
- [38] Breivik, K. et al., “Characterizing accreting double white dwarf binaries with the laser interferometer space antenna and gaia,” *The Astrophysical Journal* **854**, L1 (feb 2018).